Drift Mobilities of Electrons and Holes and Space-Charge-Limited Currents in Amorphous Selenium Films*

J. L. HARTKE†
University of Illinois, Urbana, Illinois
(Received October 11, 1961)

The band model has been applied to semiconducting amorphous selenium. Drift mobilities in pure films agreed well with previous results of Spear, and some evidence was obtained that the shallow electron and hole traps were caused by imperfections, with further considerations suggesting that the traps were distributed continuously in energy. Electron drift mobilities were reduced when arsenic was added to the films but their temperature dependence was unchanged, suggesting that arsenic increased the concentrations of imperfections which produce shallow electron traps. Hole ranges were $(2-4)\times10^{-8}$ cm²/v and exhibited no observable temperature dependence, while electron ranges were $(1-2)\times10^{-7}$ cm²/v at 300°K and decreased with decreasing temperature.

Gold and tellurium electrodes were used to inject holes into amorphous selenium, producing space-charge-limited currents at high fields. The observed currents indicated hole capture centers distributed uniformly in energy in a region extending downwards from 1 ev above the valence band edge. The densities of these levels were 10^{15} cm^{-3} ev^{-1}. Electrical conductivities of 10^{-14} to 10^{-16} ohm^{-1} cm^{-1} were obtained at low fields. The lowest value of conductivity agreed well with values extrapolated from liquid selenium. The drift of photoinjected electrons in the presence of space-charge-limited currents was used to probe the electric field. The general spatial dependence was that expected of space-charge-limiting by holes, but could not be explained quantitatively.

I. INTRODUCTION

THE electrical and optical properties[1–3] of amorphous selenium indicate that the band model of a semiconducting solid applies at least qualitatively to this noncrystalline material. The application of this model is somewhat justified[3–5] by the preservation of the short-range order of crystalline selenium in amorphous films, probably by randomly oriented chains of finite length which contain covalently bound atoms.

Many of the electrical properties have been interpreted using states in the band gap. Low, thermally activated electron and hole drift mobilities,[6] measured using bombarding electron pulses for carrier injection, have indicated high densities of shallow electron and hole traps. Other work,[7] in which carriers were injected by light pulses, has produced a higher hole drift mobility at room temperature, electron drift being unobservable in pure films, and also has indicated that the alloying of selenium with $\frac{1}{2}$ mole percent of arsenic changes electron and hole drift mobilities and ranges from those observed in pure amorphous films. Hole capture levels of moderate density and located deep in the gap have been indicated by measurements[8,9] of space-charge-limited currents[10] carried by injected holes, but an anomalous "traps-filled limit" region in the *I-V* characteristic was observed.

As in the previous work, the experiments reported here utilized injected charge carriers to examine certain regions of the band gap by transient drift mobility and steady state SCLC measurements. Measurements of drift mobilities in independently prepared films were desirable in order to obtain some indication of the origins of the shallow traps which were assumed to limit these mobilities. If impurities produce these shallow levels, then measurements on samples of various purities should result in widely varying drift mobilities. The films used in this work were vacuum evaporated onto glass substates and used high purity commercial grade selenium as well as distilled selenium which might have been relatively free of volatile impurities. Conductivity measurements suggest that both types of material were more pure than the selenium used in previous work. Anomalous differences exist between room temperature hole drift mobilities measured using light[7] and electron[6] pulses to inject carriers. Light pulses were used here to examine the discrepancy. Further examination of the effects of arsenic on carrier mobilities and ranges was warranted, particularly in view of the multiple effects previously reported, and the measurements were extended to samples of varying arsenic concentrations to permit a more meaningful interpretation of these results. Lastly, independent measurements of SCLC provided an indication of the reproducibility of the results and afforded an opportunity to examine the anomalous "traps-filled limit" region.

The effect of various distributions in energy of levels

---

* Based upon a dissertation submitted in partial fulfillment of the requirements for the Ph.D. degree at the University of Illinois, Urbana, Illinois. This work was supported by the U. S. Air Force Office of Scientific Research.

† Present address: Xerox Corporation, Rochester, New York.

[1] T. S. Moss, *Photoconductivity in the Elements* (Butterworths Scientific Publications, London, 1952), p. 185.

[2] T. S. Moss, *Optical Properties of Semiconductors* (Academic Press Inc., New York, 1959), p. 152.

[3] A. F. Ioffe and A. R. Regel, *Progress in Semiconductors* (Heywood & Company Ltd., London, 1960), Vol. 4, p. 239.

[4] A. F. Ioffe, Zhur. Tekh. Fiz. **27**, 1154 (1957) [translation: Russian Literature Survey SEM-4-57, *Soviet Progress in Semiconductors* (Infosearch Technical Information Service, London, 1957), p. 1.1].

[5] E. Mooser and W. B. Pearson, *Progress in Semiconductors* (Heywood & Company Ltd., London, 1960), Vol. 5, p. 103.

[6] W. E. Spear, Proc. Phys. Soc. (London) **B70**, 669 (1957); **B76**, 826 (1960).

[7] R. A. Fotland, J. Appl. Phys. **31**, 1558 (1960).

[8] W. E. Spear and H. P. D. Lanyon, *Proceedings of the International Conference on Semiconductor Physics, Prague, 1960* (Czechoslovakian Academy of Sciences, Prague, 1960), Paper T3.

[9] H. P. D. Lanyon and W. E. Spear, Proc. Phys. Soc. (London) **77**, 1157 (1961).

[10] The abbreviation SCLC will be used.

in the band gap on drift mobilities and SCLC will be obtained in the next section, which will be followed by a description of the experiments and the resulting population of the band gap. Although prior workers[6–9] have assumed that levels in the gap were discrete in energy, some justification will be given that a continuous distribution in energy of these states (levels separated by less than kT) may be more appropriate.

II. THEORY

A. Drift Mobilities

The time required for a thin sheet of charge carriers, produced by ionizing radiation, to drift across a biased semiconductor may be used to evaluate the carrier drift mobility. The charge of the drifting carriers is not locally neutralized when the resistivity of the semiconductor is sufficiently large, and the carrier drift induces a charge q on the plane parallel electrodes, which are separated by a distance L. For illumination through the cathode, the time dependence of the charge pulse is obtained from the relation[11]

$$dq(t)/dt=N(t)e\mu_{dn}V_0/L^2, \tag{1}$$

where $N(t)$ is the number of drifting electrons which have drift mobility μ_{dn}, and V_0 is the applied bias. If a localized state in the band gap captures a carrier after a mean free time τ_n, but releases the carrier after a time longer than the carrier transit time, the number of mobile carriers at time t after injection may be expressed as

$$N(t)=N_0\exp(-t/\tau_n), \tag{2}$$

where N_0 is the number of injected carriers. Using Eq. (2), the solutions of Eq. (1) are

$$q(t)=(N_0e\tau_n/T_{\rm tr})(1-e^{-t/\tau_n}) \tag{3}$$

for times $0<t<T_{\rm tr}=(L^2/\mu_{dn})V_0$, and

$$q=(N_0e\tau_n/T_{\rm tr})(1-e^{-T_{\rm tr}/\tau_n}) \tag{4}$$

for times $T_{\rm tr}<t\ll RC$. The charge pulse given by Eq. (3) has an approximately linear rise until time $T_{\rm tr}$, so long as $q(T_{\rm tr})>0.3N_0e$, $3\tau_n>T_{\rm tr}$, permitting the drift mobility to be evaluated. A plot of pulse height vs electric field or reciprocal transit time, when fitted to the theoretical Hecht curve of Eq. (4), permits evaluation of N_0 and τ_n. The mean distance a carrier drifts before "permanent" capture is called the Schubweg w and is given by $w=L\tau/T_{\rm tr}$. The mean distance per unit electric field is called the range r and is given by $r=\mu_d\tau$. Measurements of carrier ranges do not distinguish between traps and recombination centers, since the ultimate fate of "permanently" captured carriers is not determined.

Interpretation of the measured drift mobilities and mean free times or ranges in terms of fundamental properties of the semiconductor is strongly dependent on the assumed transport mechanism. The observed drift mobility would be the true, or microscopic, mobility if the carrier transit time were less than a mean free time before capture by a localized center, but would be less than the true mobility μ_0 if temporary trapping were important. For the case of electrons, assuming that the injected carriers and the traps are in equilibrium, then on the average, n of the carriers are free and move with the true mobility, while n_t are immobilized in traps. The drift mobility is then[12,13]

$$\mu_{dn}=\mu_{0n}n/n_t, \tag{5}$$

if $n\ll n_t$. Equation (5) may be solved explicitly for given trap distributions and positions in the energy gap. Since traps between the Fermi level and the band edge have the greatest influence on drift mobilities, the Fermi distribution function will be approximated by the Boltzmann function in this treatment. For discrete trapping levels [see Fig. 1(a)] having densities N_t, the use of Eq. (5) and its counterpart for holes give the following expressions for drift mobilities:

$$\mu_{dn}=(\mu_{0n}N_c/g_{t1}N_{t1})\exp[-(E_c-E_{T1})/kT], \tag{6}$$

$$\mu_{dp}=(\mu_{0p}N_V/g_{t2}N_{t2})\exp[-(E_{T2}-E_V)/kT]. \tag{7}$$

The degeneracy factors, g_t, may be $\frac{1}{2}$ or 2 for singly ionized donors or acceptors, and N_C and N_V are the effective densities of states in the conduction and valence bands, respectively. Thus, measurement of trap-limited drift mobilities as a function of temperature allows determination of the position of the trap relative to the band edge and, knowing the true mobility, the actual density of traps present. However, the exponential temperature dependence need not be characteristic only of a discrete trap. For the case shown in Fig. 1(b), in which there are N_t traps distributed uniformly between the band edges and cutoff energies E_T, Eq. (5) and its counterpart for holes give the

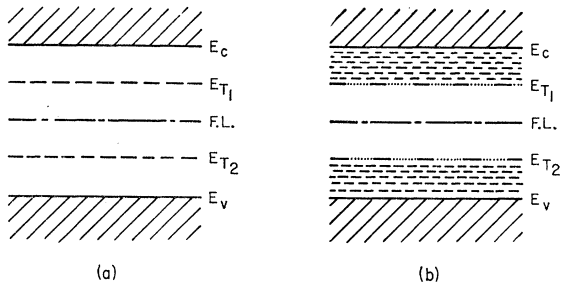

FIG. 1. Trap distributions which may limit drift mobilities. (a) Discrete trapping levels; (b) traps distributed uniformly between a band edge and a cutoff energy.

[11] F. C. Brown, Phys. Rev. **97**, 355 (1955).

[12] A. Rose, RCA Rev. **12**, 362 (1951).

[13] F. C. Brown and K. Kobayashi, J. Phys. Chem. Solids **8**, 300 (1959).

relations

$$\mu_{dn}=(\mu_{0n}N_c/g_{t1}N_{t1})[(E_c-E_{T1})/kT] \times\exp[-(E_c-E_{T1})/kT], \quad (8)$$

$$\mu_{dp}=(\mu_{0p}N_v/g_{t2}N_{t2})[(E_{T2}-E_v)/kT] \times\exp[-(E_{T2}-E_v)/kT]. \quad (9)$$

Other trap distributions having similar energy cutoffs may give pre-exponential terms of T^n. Thus, the only difference between the drift-mobility temperature dependence for discrete and continuous traps is a pre-exponential factor which might not be distinguishable over a limited temperature range, particularly since the effective densities of states and true mobilities may depend on temperature. It is clear that the specific nature of trap distributions in energy is not established by drift mobility measurements over a limited temperature range, but that a limit may be determined as to how far from the band edges the traps do extend.

Interpretation of the mean-free-time or range also depends on whether or not the drift mobility is trap limited. If the drift mobility equals the true mobility, then the observed mean free time is the true mean free time, which is often expressed as $\tau_0=(Nsv_{\text{th}})^{-1}$, where N is the available number of capturing levels, s is their capture cross section, and v_{th} is the thermal velocity of the carrier. If the drift mobility is trap limited, the observed mean-free-drift-time before "permanent" capture is greater than the true mean free time, due to the time spent in temporary traps. An analysis similar to that used[12,13] in the derivation of Eq. (5) shows that the carrier range for this case is

$$r=\mu_d\tau_d=\mu_0\tau_0, \quad (10)$$

where τ_d is the observed mean-free-drift-time before "permanent" capture of a carrier. Thus the range possesses greater significance than does the mean-free-drift-time. The model of trap-limited drift mobilities will be applied to the experimental results in Sec. IV (A).

B. Space-Charge-Limited Currents

When ohmic contacts are made to a high-resistivity semiconductor, injected carriers may result in currents far in excess of ohmic currents, and the space charge of injected carriers limits the current. The theory of SCLC is well established,[14–16] and this discussion will follow the semiquantitative approach of Rose.[15]

For a semiconductor of thickness L, having plane parallel electrodes, into which the positive electrode can freely supply holes while the cathode is blocking for electrons, a one-carrier SCLC exists when the density of injected holes is much greater than thermal equilibrium carrier densities. The injected space charge per unit area, Q, is

$$Q\approx\epsilon V/L \quad (11)$$

when a voltage V is applied, ϵ being the dielectric constant of the semiconductor. The injected carriers move across the semiconductor in a time $T_{\text{tr}}\approx L^2/\mu_0 V$ if trapping of the injected carriers is insignificant, μ_0 being the true hole mobility, producing a current density

$$j=Q/T_{\text{tr}}\approx\epsilon\mu_0 V^2/L^3. \quad (12)$$

The V^2 dependence of current on voltage and the use of true mobility are characteristic of SCLC in a trap-free solid. If electronic states are present in the band gap, then only the fraction $p/(p_t+p)$ of the injected carriers are free to conduct, p and p_t being the densities of holes in the valence band and in hole-capture centers, respectively. Thus, when the rate of exchange of carriers between the band and capture centers has reached the steady state, and if the inequality, $p_t\gg p$, holds, the current is

$$j\approx(\epsilon\mu_0 V^2/L^3)(p/p_t). \quad (13)$$

For states of density N_t at a discrete energy E_T in the band gap, the SCLC from Eq. (13) is

$$j\approx(\epsilon\mu_0 V^2/L^3)(N_v/N_t)\exp[-(E_T-E_v)/kT)], \quad (14)$$

if the states lie between the hole quasi-Fermi level and the valence band such that Boltzmann statistics apply. More holes are injected as the voltage is increased, the numbers of free and trapped holes increase, and the quasi-Fermi level for holes moves toward the valence band. This level will pass through the discrete level at a sufficiently high applied voltage, and all charge injected hence will remain free, causing a steep rise in current referred to[16] as the "traps-filled limit," in which the current approaches the trap-free current predicted by Eq. (12). The latter is rarely obtained in practice as the applied voltage is limited by the breakdown field or the heating effects of the high currents involved.

A significantly different type of current-voltage relation exists if the thermal equilibrium Fermi level $\bar{E}_F$ lies in the midst of a uniform distribution in energy of hole capture centers of density η_t per unit volume per unit energy. If the applied voltage moves the hole Fermi level a distance δE from $\bar{E}_F$ towards the valence band, then one obtains

$$p/p_t=(\bar{p}/\eta_t\delta E)\exp(\delta E/kT). \quad (15)$$

The relation between δE and the applied voltage V may be obtained from Eq. (11):

$$Q\approx\epsilon V/L\approx eLp_t\approx eL\eta_t\delta E. \quad (16)$$

Using these two relations, the SCLC from Eq. (13) is then

$$j\approx(\bar{p}e\mu_0 V/L)\exp(\epsilon V/eL^2\eta_t kT). \quad (17)$$

If the semiconductor is p type, the pre-exponential

[14] W. Shockley and R. C. Prim, Phys. Rev. **90**, 753 (1953).
[15] A. Rose, Phys. Rev. **97**, 1538 (1955).
[16] M. A. Lampert, Phys. Rev. **103**, 1648 (1956).

term is ohmic, being the current expected in the absence of space-charge limiting.

A current-voltage behavior which includes both V^2 and $V\exp(V/V_0)$ regions is obtained for the case of a uniform distribution of hole capture centers several kT below the thermal equilibrium Fermi level. If there are η_t of these levels per unit volume per unit energy between energies E_T and $E_T-\Delta E$ in the band gap, the SCLC for $E_{Fp}>E_T+2kT$ is then

$$j\approx(\epsilon\mu_0V^2/L^3)(N_v/kT\eta_t)\exp[-(E_T-E_v)/kT] \quad (18)$$

if $\Delta E>3kT$, being similar to that given in Eq. (14), while for $E_T-2kT>E_{Fp}>E_T-\Delta E+2kT$ the SCLC is

$$j\approx N_v\exp[-(E_T-E_v)/kT](e\mu_0V/L)\times\exp[\epsilon V/eL^2\eta_tkT], \quad (19)$$

which is similar to Eq. (17). The current-voltage characteristic obtained for this case could easily be mistaken as being due to a discrete level, since the rapid rise in current with increasing voltage predicted by Eq. (19) might appear to be the traps-filled limit.[16] For other continuous distributions of levels in energy, Eq. (19) would have the form $j\propto V\exp(V/V_0)^n$.

Thus, SCLC measurements enable the densities and energy distributions of states which are near the thermal equilibrium Fermi level to be explored, as these levels generally contain the majority of trapped carriers, and complement measurements of trap-limited drift mobilities, which are often affected by states near a band edge, these states being present in greater number than the deep levels.

When the current is space-charge limited, the electric field in the semiconductor is nonuniform,[15] being small at the injecting contact where the space charge density is large and rising to $V/L<E<2V/L$ at the other contact.[16] The technique of drift mobility measurement affords an opportunity to probe the spatial dependence of this electric field. The velocity of drifting carriers, which is directly related to the shape of the leading edge of the charge pulse, is proportional to the electric field, the constant of proportionality being the drift mobility. In general, the Fermi level will be near states deep in the gap, thus the drift mobility, limited by shallow traps, will be constant throughout the majority of the semiconductor. Using Eq. (2), and recognizing the presence of the nonuniform field, the pulse shape from Eq. (1) is

$$dq(t)/dt=(N_0e\mu_d/L)E(t)\exp(-t/\tau), \quad (20)$$

and enables the electric field in the semiconductor to be evaluated directly from the pulse shape in terms of the time during which the carriers have drifted. The spatial dependence of this electric field may be obtained by using the relation

$$x=\int_0^t\mu_dE(t')dt', \quad (21)$$

which relates the distance traveled by the sheet of carriers to the drift time. The model of trap-limited SCLC will be applied to the experimental results in Sec. IV (B).

III. EXPERIMENTAL TECHNIQUES

A. Sample and Sample Holder

The amorphous selenium films used in this work were prepared[17] by vacuum evaporation onto glass substrates which were approximately 1-in. square and $\frac{1}{16}$-in. thick, and which had previously been coated with tin oxide (NESA)[18] to provide an optically transparent, conductive coating. The over-all evaporation times were about 20 min, during which the substrate temperatures were in the 55 to 65°C range, producing 20-μ thick amorphous selenium films which were 1.5-cm square.

Four different types of films were investigated, the first using commercial, or xerographic, grade selenium supplied by Canadian Copper Refiners. The result of a spectrographic analysis performed by the supplier on a typical batch of this material is shown in Table I. The second type of film utilized selenium which had been triply distilled in vacuum by the writer and was kept in vacuum until evaporation onto substrates, hopefully freeing the selenium of some volatile contaminants. The techniques of distillation are subsequently described. The impurities present before and after distillation, obtained by spectrographic analyses performed by Canadian Copper Refiners, are listed in Table I and indicate that the triply-distilled selenium contained about the same amount of nonvolatile impurities as the presently available commercial grade, which was not available at the time the distillation was performed. The third type of film was prepared from selenium alloyed with 0.5 mole percent of arsenic, and the fourth with 2 mole percent As. The selenium, alloyed with As, was obtained from Horizons, Inc. and was evaporated from a single crucible. A spectrographic analysis of its impurity content was not made.

The tin oxide coating was consistently used as one electrical contact to the film, but the material used for the other contact varied. A hole-injecting contact was provided by a 1-cm square gold contact evaporated onto the film or by a thin (several thousand A) layer of Te. As the nonuniform electric field caused by injection was undesirable for drift mobility measurements, a thin (approximately 2000 A) layer of ZnS was used to provide a blocking electrode. One-cm square gold contacts were evaporated onto the Te and ZnS layers.

The vacuum distillation techniques used were identical to those reported by Humphrey,[19] with the exception that the distillation was performed in a

[17] All samples were supplied by the Xerox Corporation and were prepared by W. J. Murphy, the electrode materials being suggested by M. Levy.

[18] A trademark of the Pittsburgh Plate Glass Company.

[19] J. N. Humphrey, Naval Ordnance Laboratory Report NAVORD-3922 (unpublished), Chap. III.

TABLE I. Impurities in selenium from spectrographic analyses.

Impurity[a]	Concentration[b] (ppm) Commercial grade	Distilled before	Distilled after	Detection limit (ppm)
Te	2–3	≈15	2	...
Fe	ND	6	ND	2.0
Cu	0.06–0.08	0.2	0.08	0.1
Cd	ND	BV	ND	0.5
Mg	1	T	ND	1.0
Si	ND	BV	1	1.0

[a] The following impurities were not detected: Pb, Bi, Ag (0.5 ppm detection limit), Hg, Sb, Sn, Ni, Cr, Al, In (1.0 ppm detection limit), As, Ti (2.0 ppm detection limit), Na (3.0 ppm detection limit), Zn (6.0 ppm detection limit).
[b] ND = not detected, BV = barely visible, T = trace, and ppm = parts per million.

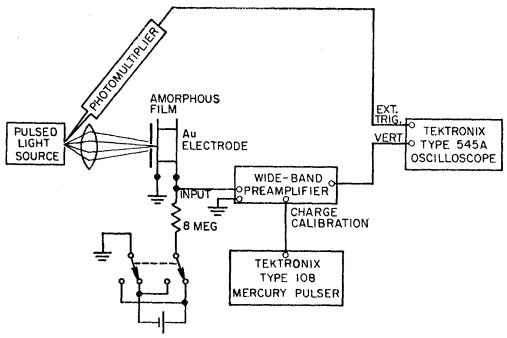

FIG. 2. Experimental arrangement used for the measurement of drift mobilities.

quartz tube, since selenium has been found[20] to absorb some of the constituents of glass (particularly boron). The melting point of selenium being 217°C, the selenium was evaporated at 250°C to prevent the evaporation of nonvolatile impurities and was condensed at 200°C to prevent collection of volatile impurities.

The sample was mounted on a copper heat sink, the NESA electrode being electrically and thermally connected to the sink. Electrical contact to the gold electrode was made by a spring clip which was insulated from the sink by a teflon spacer; the leakage resistance was approximately 10^{15} ohms. The sample and sink were mounted in an evacuated container. A window in the wall of the container allowed the film to be illuminated through the NESA electrode. All but a 0.2-cm^2 area of this electrode directly under the gold contact was masked to insure that photoinjected carriers would drift in a region of uniform electric field. The copper heat sink was cooled with dry nitrogen gas which had been precooled to liquid N_2 temperatures. The sample temperature, measured by a copper-constantan thermocouple calibrated to ±0.3°, could be varied between room temperature and 90°K by control of the precooled dry N_2 flow rate and could be maintained to within ±0.5° or better for one hour.

B. Drift Mobilities

Drift mobilities of electrons and holes in amorphous selenium films were measured using the arrangement shown in Fig. 2. A sheet of $1–2\times10^8$ electron-hole pairs was created in the amorphous film at the tin oxide electrode by a 10-nsec light pulse which was optically focused on the transparent electrode. The sample was thoroughly shielded from ambient illumination to prevent secondary photoeffects. Since the optical absorption coefficient of amorphous selenium is greater than 10^4 cm^{-1} in the range in which there is appreciable photoresponse,[2] causing the pairs to be created in a distance from the transparent electrode which was less than 2% of the film thickness, and since the duration of the light pulse was much less than the shortest carrier transit time (0.15 μsec), the thickness of the sheet of injected carriers was much less than the film thickness. The 8-megohm resistor effectively isolated the battery supply from the equivalent ac circuit, but affected the voltage across the sample a negligible amount as the sample resistance was greater than 10^9 ohms. The drift of either electrons or holes could be observed by choosing the polarity of the battery supply.

The transient voltage across the film, produced by the drift of injected electrons or holes, was amplified by a wide-band preamplifier having a voltage gain of 10, and was observed as vertical deflection on the screen of a Tektronix type 545A oscilloscope which had a type L plug-in unit. The frequency response of the combination had −3 db points at 60 cps and 25 Mc/sec, giving a rise time of 18 nsec and a low frequency time constant of 1.5 msec. The rise time was much less than the shortest carrier transit time. The input impedance of the wide-band preamplifier was 3 megohm, and the internal noise was less than 20 μv peak-to-peak referred to the input with grounded input. With the circuit shown in Fig. 2, electron drift produced a downward, or negative, vertical deflection on the oscilloscope screen, holes giving positive deflection. The horizontal sweep of the oscilloscope was initiated by the light pulse via a 1P21 photomultiplier. The time dependence of the voltage across the film was recorded by photographing the pulse observed on the oscilloscope screen; three pulses were recorded for each carrier at each temperature and voltage. The horizontal sweep rate of the oscilloscope was calibrated to ±3% using time-mark generators. The vertical deflection of the oscilloscope was calibrated to ±10% in terms of charge by applying a voltage step function of known amplitude from a mercury pulser to the input of the wide-band preamplifier through a 1 picofarad capacitor. The preamplifier-oscilloscope combination had a maximum sensitivity of 0.5 mv/cm, and the total capacity shunting the sample electrodes was approximately 300 picofarads. Thus, the drift of about 10^6 electronic charges or 10^{-13} coul could be detected. As the effective resistance shunting the sample was 2 megohm, neither the resulting time constant of 600 μsec nor the 1.5-msec

[20] F. Eckart, Ann. Physik 14, 233 (1954).

time constant of the preamplifier produced serious distortion of the drift pulses at the maximum observed drift time of 60 μsec.

The pulsed light source utilized two air spark gaps in series which were triggered to generate fast light pulses; the repetition rate could be varied from manual operation to 1000/sec. A 100-picofarad capacitor, charged to 4.5 kv, was discharged through the gaps by the triggering action of a hydrogen thyratron, using a circuit which has been previously described,[21] in which the thyratron and its associated inductance was removed from the main discharge path. The actual half-width of the light pulse was approximately 10 nsec and the 10%-width was about 30 nsec. Although a keep-alive electrode was used to stabilize the discharge, the number of carriers injected by each pulse varied by about 40%. Thus, drift pulse heights were obtained by visually averaging 20 to 100 pulses.

C. Space-Charge-Limited Currents

Steady-state, direct currents were produced and measured by the series connection of a battery supply, the sample, and an Applied Physics Corp. model 31 vibrating reed electrometer. The currents were measured by connecting calibrated high-value resistors between the insulated input and feedback terminals of the electrometer. The voltage drop across its input terminals was always much less than the voltage applied to the sample. The accuracy of the current measurement was 10% for currents between 10^{-14} and 10^{-6} amp. As gold and tellurium contacts are capable of injecting holes into amorphous selenium,[9] the polarity of these contacts was positive with respect to the NESA contact in order to produce one-carrier SCLC. The applied voltage was cycled over its range several times to assure reproducibility. The maximum applied voltage was limited by the breakdown field of amorphous selenium,[9] which is about 4×10^5 v/cm. Since amorphous selenium is photoconductive, the sample was thoroughly shielded from ambient illumination.

IV. EXPERIMENTAL RESULTS

Certain parameters of amorphous selenium were used in the interpretation of all data. As measurements of true mobilities are nonexistent, the values used by Spear[6,8] of $\mu_{0n}=10$ cm^2/v sec and $\mu_{0p}=60$ cm^2/v sec were used for the sake of consistency. These mobilities were assumed to be temperature independent. A ratio of effective mass to free-electron mass of 2.5 was used for electrons and holes, giving effective densities of states $N_c=N_v=10^{20}$ cm^{-3} at 300°K. The effective mass which was used for holes has been obtained from Faraday rotation.[2] A dielectric constant of 6 relative to air was used.

A total of 12 amorphous selenium films were investigated. The significant chemical and physical properties of these films are given in Table II.

TABLE II. Properties of the amorphous selenium films used in this investigation.

Film No.	Purity	Electrodes	Thickness (microns±7%)
I	Commercial grade	NESA, Au	21.5
II	Commercial grade	NESA, Au	21.5
III	Commercial grade	NESA, ZnS-Au	21.3
IV	Commercial grade	NESA, ZnS-Au	21.3
V	Distilled	NESA, ZnS-Au	21.3
VI	Distilled	NESA, ZnS-Au	21.3
VII	Commercial grade	NESA, ZnS-Au	23.7
VIII	0.5 mole percent As	NESA, ZnS-Au	21.3
IX	0.5 mole percent As	NESA, ZnS-Au	21.3
X	2 mole percent As	NESA, ZnS-Au	20
XI	2 mole percent As	NESA, ZnS-Au	20
XII	Commercial grade	NESA, Te-Au	21.3

A. Drift Mobilities

Drift mobilities of electrons and holes were measured in the 220–300°K temperature range. Measurements were not taken at higher temperatures because of possible crystallization, nor were they possible at lower temperatures due to effects of "permanent" trapping. As the spark source produced light throughout the visible and ultraviolet region, the dependence of carrier transit times on incident photon energies was investigated by attenuating photons having energies less than 2.1 ev and greater than 2.6 ev with glass color filters. The filtering had no observable effect on carrier transit times but indicated that photons having energies greater than 2.5 ev produced the majority of electron-hole pairs. The transit times were likewise independent of the total number of photoinjected pairs throughout the 10^6–10^8 carriers/pulse range; thus, maximum intensity of the light pulse was used to provide a large signal to noise ratio.

If the sample was illuminated with more than 10^2–10^3 light pulses during the drift of one carrier and was then electrically shorted, drift pulses were observed which corresponded to carriers of opposite charge. This effect has been attributed[6] to polarization of the sample which is caused by capture of the drifting carrier by deep levels; the resulting space charge then attracts carriers of opposite charge. Since such a space charge would produce erroneous transit time and pulse height data, the following steps were taken to prevent polarization. Before each measurement the shorted sample was illuminated with 1000 pulses per second from the light source; any polarization effects then rapidly disappeared. The light source was then turned off and voltage was applied to the sample, after which the measurements were made.

No physical changes were observed in films cooled from room temperature to −20°C so long as the cooling rate did not exceed 20 deg/hr. However, small, localized sections of the films would pull away from the glass

[21] A. Bardocz and A. Klatsmanyi, Rev. Sci. Instr. **26**, 945 (1955).

substrates at lower temperatures, forming small bubbles, and large sections of the films shattered and peeled away from the substrates below −35°C. The strain-induced damage was probably caused by a large difference between the temperature coefficients of expansion of amorphous selenium and glass, as no such damage was mentioned by Spear[6] who used mica substrates. The illuminated portions of shattered films were held in place by the clip which provided electrical contact to the gold electrode and room temperature mobilities were reproducible, even if 70% of the film had fallen off the substrate. However, carrier ranges were not reproducible after the films broke and indicated that a large number of deep capture levels for electrons and holes had been introduced. These levels could have been surface states, since cracks were observed in the illuminated portion of the film.

The drift of carriers in pure films which had ZnS blocking electrodes produced linearly rising pulses with a sharp corner at the time of injection. However, the pulse was rounded when the carriers were collected, this portion occupying about 15% of the total transit time; this effect was previously reported by Spear.[6] In practice, the two linear portions near the rounded region were extrapolated and their intersection was taken to be the actual time of collection. This absence of a well-defined corner may be interpreted as an increase with time of the carrier-sheet thickness, probably caused by diffusion and by the statistical nature of the trapping and release of carriers. A space-charge region near the collecting electrode could also account for the effect, as could small variations in the film thickness. The drift of holes in film II, which had a gold collecting electrode, produced hole pulses as described above, but the pulses due to electron drift were distorted. This distortion will be examined in Sec. IV (B).

The drift of holes in films which contained 0.5 and 2 mole percent arsenic produced pulses similar to those observed in pure films, but electron pulse shapes differed considerably. An electron pulse typical of 0.5 mole percent As films is shown in Fig. 3 and consists of an

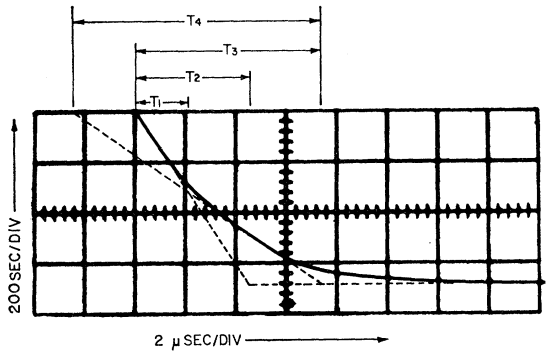

FIG. 3. Pulse shape due to drifting electrons in an amorphous selenium film containg 0.5 mole percent arsenic. Film VIII; $T=297°K$; electric field, $E=8.6\times10^4$ volts/cm.

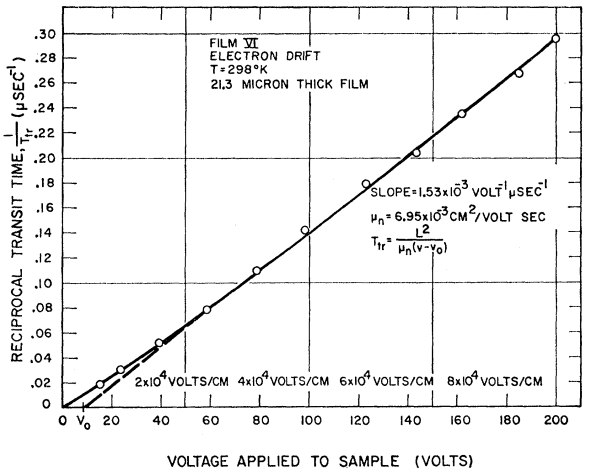

FIG. 4. Graphical method used for the evaluation of drift mobilities.

initial, fast, linear rise followed by a final region in which the voltage changes more slowly with time. As blocking ZnS layers were used and since hole pulse shapes indicated a uniform electric field, the electron pulse shape indicates that the mobility of the electrons was not constant throughout the sample. If the assumption is made that two different layers, each homogeneous, existed in series between the electrodes, then time T_2 would approximate the transit time of electrons across the film if it consisted entirely of the material which comprised the layer nearest the NESA electrode. Similarly, T_4 would approximate the transit time of electrons in an entire film of the second layer. However, if two different regions existed in parallel between the electrodes, time T_1 would be the transit time of "fast" electrons and time T_3 would be that of "slow" electrons. The initial, linear rise in time T_1 was replaced by a small, curved region in films containing 2 mole percent As, and times T_1 and T_2 were not distinguishable. Electron drift times T_3 and T_4 could be resolved, T_4 being only 30% greater than T_3.

Hole and electron drift mobilities were evaluated by plotting reciprocal transit times, obtained from photographed pulses, vs voltage and by fitting the high-field points to a straight line, as shown in Fig. 4. The intercept of this line at V_0 on the voltage axis, also reported by Spear,[6] was 0 to 20 v for undamaged films, but values up to 50 v were obtained after the films shattered at low temperatures; no significant temperature dependence was observed. This voltage could be due to rectifying contacts. The possible error in evaluation of the drift mobilities was 10%, being primarily limited by the rounded collecting edge and by pulse distortion, described by Eq. (3), at low fields.

The resulting drift mobilities in films of distilled and commercial grade selenium are shown in Fig. 5. The temperature dependence of hole mobility was $\exp(-0.14\ \text{ev}/kT)$, and that of electrons was

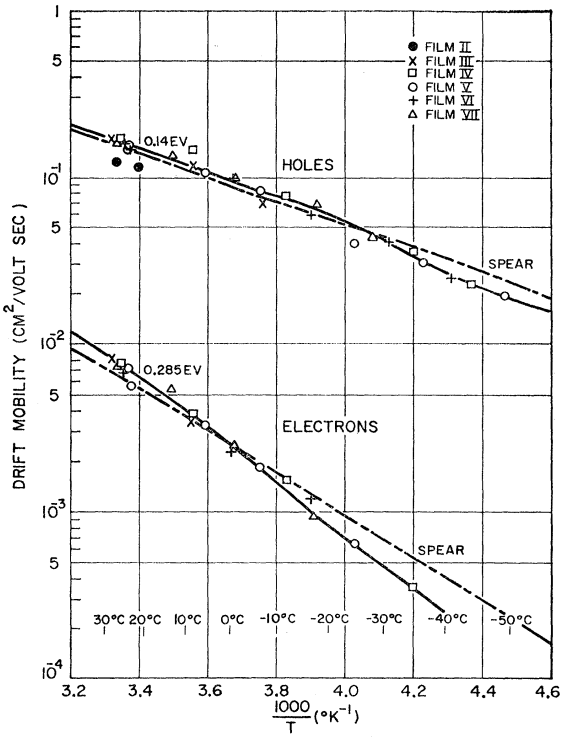

FIG. 5. Electron- and hole-drift mobilities in pure amorphous selenium films.

$\exp(-0.285\ \text{ev}/kT)$. If a pre-exponential term of T^n was present, the data suggest $-2<n<2$. Drift mobilities at 300°K were 0.165 cm²/v sec for holes and 7.8×10^{-3} cm²/v sec for electrons. The values obtained for holes are in excellent agreement with Spear,[6] while the electron drift mobilities differ slightly from his results.

At temperatures near −30°C for holes and near −12°C for electrons, the drift mobilities anomalously decreased, but again took up the high-temperature dependence at lower temperatures. The temperatures at which the anomalies occurred show some correlation with those at which physical damage occurred, and it is proposed that structural changes in the films account for the anomalous reductions of mobility. These changes could not have been of a permanent nature, however, since room temperature mobilities were reproducible. A decrease in true carrier mobility, due to scattering from the structural changes, would account for the anomalies, as would the introduction of shallow traps of the same nature as those which limit the mobilities in unstrained films. This experiment is incapable of selecting one of the two models, but the results do indicate that two different types of structural imperfections exist, one affecting hole and the other electron mobilities, as the anomalies occurred at different temperatures for holes and electrons.

The high-temperature behavior of the drift mobilities was interpreted using the trap-limiting model. Assuming discrete trapping levels as shown in Fig. 1(a), Eq. (6) gives a shallow electron trap density of $N_{t1}=4\times10^{18}$ cm^{-3} with $g_{t1}=\frac{1}{2}$ (singly ionized acceptors), and Eq. (7) gives a shallow hole trap density of $N_{t2}=3.3\times10^{20}$ cm^{-3} with $g_{t2}=\frac{1}{2}$ (singly-ionized donors). The data may be interpreted equally well by assuming a uniform distribution of traps between each band edge and a cutoff energy, as shown in Fig. 1(b). This case gives $N_{t1}=4.4\times10^{19}$ cm^{-3} and $N_{t2}=1.8\times10^{21}$ cm^{-3} from Eqs. (8) and (9), respectively, again with $g_{t1}=g_{t2}=\frac{1}{2}$. The temperature dependences of the drift mobilities give $E_c-E_{T1}=0.285$ ev and $E_{T2}-E_v=0.14$ ev for either of the two models shown in Fig. 1. Some justification for the above assignments of donor and acceptor properties to the hole and electron traps respectively will be given in Sec. V.

Drift mobilities obtained in amorphous selenium films which contained large amounts of arsenic are shown in Fig. 6. Hole mobilities in those films which contained 0.5 mole percent As agree with those observed in pure films, while mobilities in 2 mole percent As films are slightly lower, probably being caused by a decrease in true hole mobility due to impurity scattering. Thus, the addition of arsenic produced no change in the number or position in the band gap of the shallow hole traps. However, a significant effect on electron drift mobilities did occur upon the addition of arsenic. Electron drift mobilities, shown in Fig. 6, were evaluated on the basis of the series-layer model. The initial

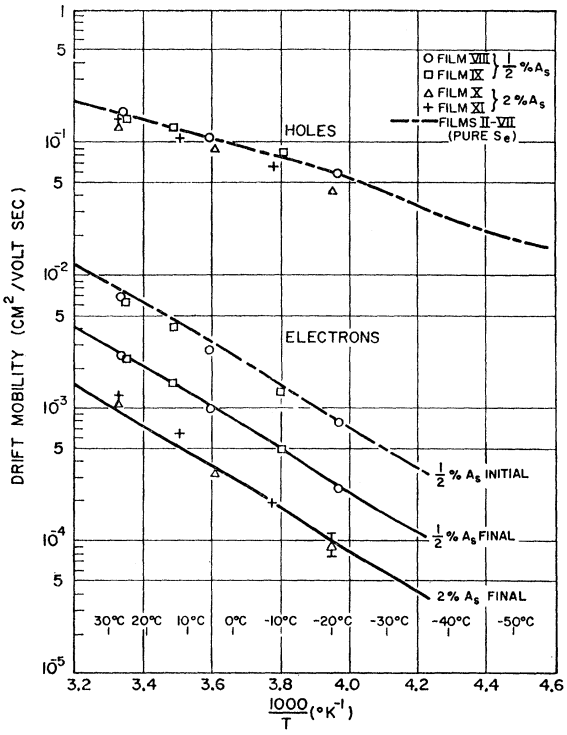

FIG. 6. Electron- and hole-drift mobilities in amorphous selenium films containing arsenic.

mobilities in 0.5 mole percent As films agree quite well with those observed in pure films, while the final mobilities are smaller by a factor of 3, decreasing still further with the addition of 2 mole percent As to the selenium. At 300°K, the final electron drift mobility was 2.6×10^{-3} cm²/v sec in films containing 0.5 mole percent As, and was 9.3×10^{-4} cm²/v sec in 2 mole percent As films. The temperature dependence of electron drift mobility was unaffected by the addition of arsenic. If the pulse shape was interpreted using the parallel-region model, the temperature dependence was unchanged. In 0.5 mole percent As films the "fast" electron mobility was 1.7×10^{-2} cm²/v sec at 300°K, while the "slow" electron mobility was 4.4×10^{-3} cm²/v sec; the two values bracketed the mobility in pure films. At 300°K, the "slow" electron drift mobility was 1.4×10^{-3} cm²/v sec in 2 mole percent As films.

Since the selenium and the arsenic were evaporated from a single crucible, it is likely that the initial vapor was almost pure selenium, and that arsenic evaporated only during the latter part of the evaporation. The initial electron drift mobility in 0.5 mole percent As films, obtained using the series-layer model, and the reduction of the initial region of the drift pulse when 2 mole percent of As was introduced support this proposal. Thus, it is believed that the model of a pure layer in series with a layer containing about the specified amount of arsenic is valid. The thickness of the pure layer, obtained from the ratio of T_1 to T_2 (Fig. 3), was 40% of the total film thickness in 0.5 mole percent As films.

The results indicate that arsenic produces shallow electron traps when introduced into amorphous selenium. A plot of reciprocal final electron-drift mobility at 300°K vs arsenic concentration gave a nearly linear relation between the points of 0, 0.5, and 2 mole percent As, the $1/\mu=0$ intercept being near -0.25 mole percent. If the number of shallow electron traps introduced by the arsenic was equal to the arsenic concentration, then the relation $1/\mu \propto (N_t+N_{As})$ would be expected, N_t being the density of shallow electron traps which were present in pure material. The $1/\mu=0$ intercept then gave $N_t\approx8\times10^{19}$ cm^{-3} if a density of 4.3 g cm^{-3} was used for amorphous selenium. This trap density was higher than those obtained for pure films, but is in satisfactory agreement, considering the inhomogeneous nature of the As alloy films and the assumptions required to calculate a trap density in pure films.

It is quite doubtful that the trapping levels produced by the arsenic were due to the capture of an electron at the site of an arsenic atom, since the position in the energy gap of these trapping levels was unchanged by the addition of As, as seen from the temperature dependence of the electron-drift mobility. If, as proposed,[7] trivalent arsenic substitutionally enters a chain of divalent Se atoms and crosslinks chains by means of the extra p electron, the resulting incorrect bond

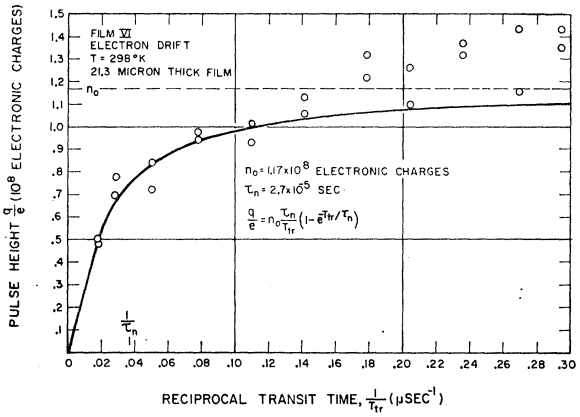

FIG. 7. Hecht curve of a typical measurement.

angles in the chain would decrease the order of the film. The density of structural imperfections would therefore increase, giving an increase in the density of shallow electron traps arising from a type of structural imperfection. This interpretation is somewhat supported by the anomalous decrease in electron mobility which occurred when pure films were strained.

The mean-free-drift times of the carriers before "permanent" capture were obtained by plotting the observed pulse heights vs reciprocal transit times on a log-log scale. The data were then fitted to the theoretical curve, given by Eq. (4), which was plotted on an identical scale using reduced variables. A typical fit, shown in Fig. 7, indicates that the amplitude jitter of the light pulse prevented the accurate measurement of mean-free-drift times. The range of each carrier was obtained by taking the product of resultant mean-free-drift times and drift mobilities, each measured simultaneously in a film at each temperature.

Mean-drift times and ranges for holes in amorphous films of commercial grade selenium are shown in Fig. 8. Those observed in distilled and arsenic alloy samples were similar. The hole range in distilled material was about 3.5×10^{-8} cm²/v, while that in films containing arsenic averaged 1.8×10^{-8} cm²/v. Although the scatter was quite large, the results indicate that the hole range does not depend strongly on temperature. This would suggest that the number of deep capture centers for holes, obtained from Eq. (10), did not depend significantly on temperature, since μ_0, s, and v_{th} would not be expected to give a large temperature dependence.

Electron ranges, shown with mean-free-drift times in Figs. 9 and 10, did exhibit a strong dependence on temperature, which indicates that the number of deep-electron-capture centers increased as temperature decreased. Since amorphous selenium is probably p type, the thermal equilibrium Fermi level would be expected to move toward the valence band as temperature decreased, ionizing any donor levels it passed through and making them active electron capture centers. As no unique electron transit time existed in

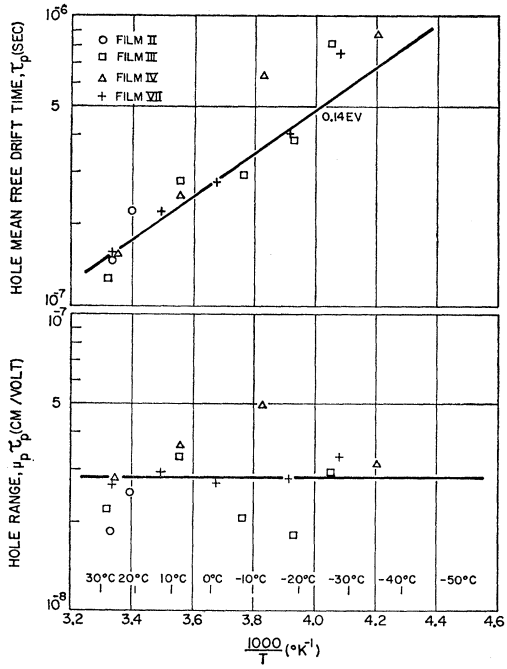

FIG. 8. Temperature dependences of hole mean-free-drift time and range in amorphous films of commercial grade selenium.

the As alloy films, plots of pulse height vs applied voltage were used to obtain electron ranges characteristic of the material at room temperature. Films VIII-XI consistently gave an electron range of $(3.1\pm0.2)\times10^{-8}$ cm²/v.

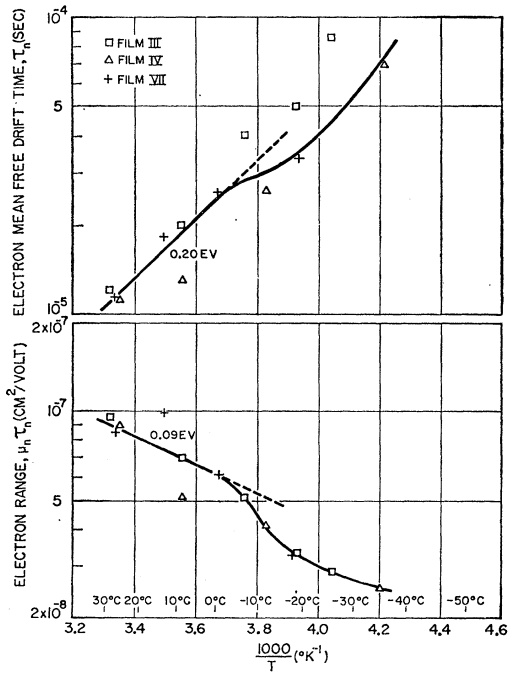

FIG. 9. Temperature dependences of electron mean-free-drift time and range in amorphous films of commercial grade selenium.

Thus, hole and electron ranges were slightly greater in films prepared from distilled material than in those utilizing commercial grade selenium and were smaller in films which contained arsenic. The actual concentration of arsenic had no effect on the ranges, indicating that the smaller ranges in As alloy films were characteristic of the selenium to which the arsenic had been added. As the nonvolatile impurity concentrations of commercial grade and distilled selenium were nearly identical, the deep electron and hole capture centers are likely due to volatile impurities.

B. Space-Charge-Limited Currents

Steady-state direct currents were measured over a wide range of applied voltages for three amorphous

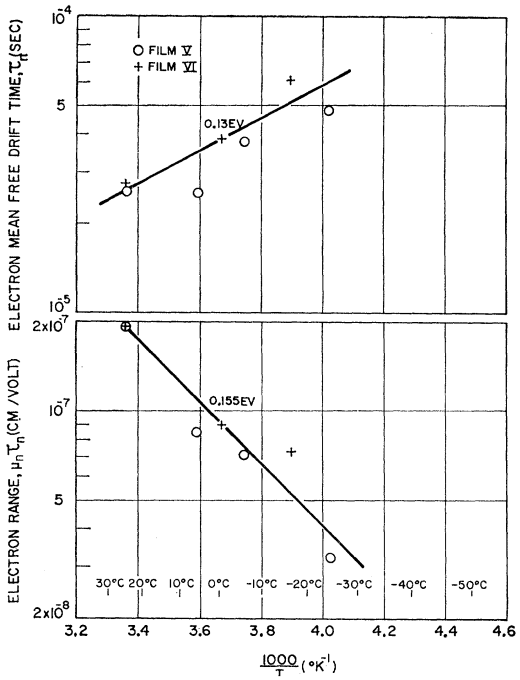

FIG. 10. Temperature dependences of electron mean-free-drift time and range in amorphous films of distilled selenium.

selenium films. When the applied voltage was increased in the SCLC range, the current decreased towards its steady state value, while if the voltage was decreased, the current increased with time. This behavior is characteristic of SCLC and is due to the time required for centers to capture or release carriers. If a forming process, reported previously,[9] was required to produce injecting contacts, the forming occurred within a few hours after the voltage was first applied, that being the time required to establish a steady-state condition; this several-hour wait was required at all voltages.

The dependences of current on voltage for the three films are shown in Figs. 11 and 12, and an expansion of the high voltage region of film XII is shown in Fig. 13. The functional relations between current and voltage

which were used to fit various portions of the *I-V* characteristics are also shown in the figures. The measurements were made at a mean room temperature of 297°K, with a daily fluctuation of ±2° accounting for some of the scatter.

For applied voltages greater than 1 v, the dependence of current on voltage for film I was of the form predicted by Eq. (17), the thermal equilibrium Fermi level being in a uniform distribution of hole capture centers. The *I-V* curve for film II is similar to that of film I for V greater than 10 v, but the dependence of current on

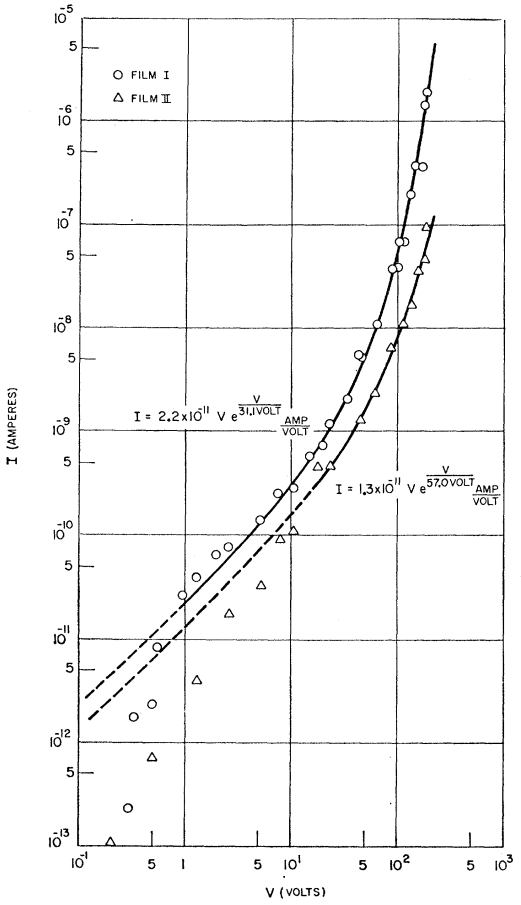

FIG. 11. Space-charge-limited currents in amorphous selenium films having gold hole-injecting contacts.

voltage was between V and V^2 at lower voltages. This suggests that the thermal equilibrium Fermi level was less than kT above a uniform distribution of hole capture levels, and that Eq. (19) applies to the high voltage region. For voltages less than 10 v the current was probably a mixture of ohmic and SCLC. At less than 1 v, both films suggest the presence of a forward-biased rectifying contact. However, no simple relation of the type $I \propto V - V_0$ was capable of fitting the data in that region.

Film XII, which utilized a Te anode, did permit such

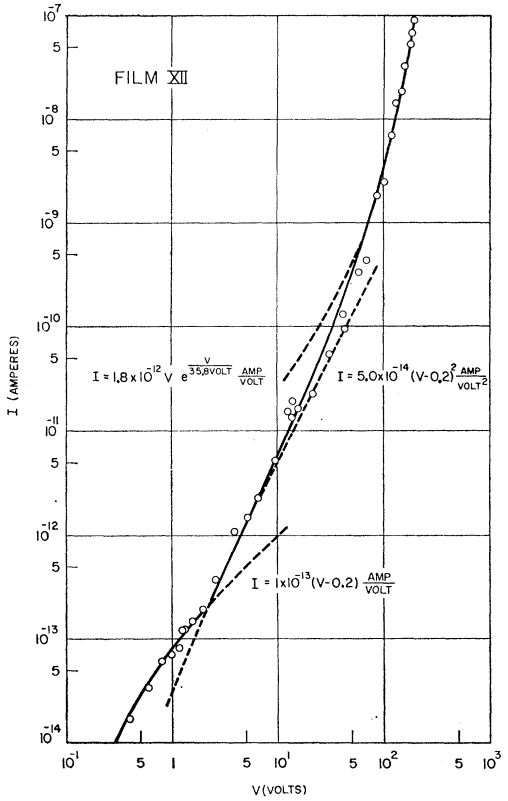

FIG. 12. Space-charge-limited currents in an amorphous selenium film having a tellurium hole-injecting contact.

a fit in the low voltage region, which suggests that the NESA cathode was a forward-biased rectifying contact. The I-V characteristic of this film, shown in Figs. 12 and 13, indicates that the thermal equilibrium Fermi level was several kT above a uniform distribution of hole capture centers. Below 2 v the current followed Ohm's law, $j = \bar{p}e\mu_{0p}V/L$, while between 2 and 20 v,

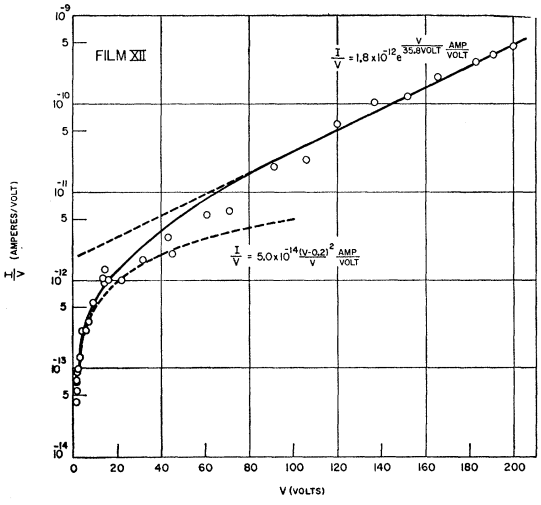

FIG. 13. Expanded high voltage region of Fig. 12.

TABLE III. Electrical properties of the amorphous selenium films determined from space-charge-limited current measurements.

Film No.	dc conductivity $\sigma=\bar{p}e\mu_{0p}$ (ohm^{-1} cm^{-1}, ±30%)	$\bar{p}$ (cm^{-3}, ±30%)	$\bar{E}_F-E_V$[a] (ev, ±1%)	E_T-E_V[b] (ev, ±1%)	η_t[c] (cm^{-3} ev^{-1}, ±20%)
I	4.7×10^{-14}	4900	0.96	>0.98	8.7×10^{14}
II	···	···	0.97<, <1.0	0.97	1.6×10^{15}
XII	2×10^{-16}	21	1.10	1.03	1.0×10^{15}

[a] Position of the thermal equilibrium Fermi level relative to the valence band edge.
[b] Position of the upper edge of the uniform distribution in energy of hole-capture levels relative to the valence band edge.
[c] Density of the uniform distribution in energy of hole-capture levels.

before the quasi-Fermi level for holes entered the trap distribution, the current was of the form predicted by Eq. (18). The solid curve in this region was calculated using Eqs. (11), (13), and the Fermi distribution function rather than the Boltzmann approximation. Although the fit is not entirely satisfactory between 20 and 80 v, the discrepancies are not serious, since at these voltages the quasi-Fermi level for holes was just entering the trap distribution. As the theoretical curves were obtained with the assumption of a "sharp" edge for the uniform trap distribution in energy, a diffuse edge would cause the observed currents to be slightly less than those predicted. At applied voltages greater than 80 v, the current was of the form predicted by Eq. (19). It should be noted that the parameters η_t and E_T-E_v both occur in Eqs. (18) and (19) and that the fits to the experimental points in the two regions are not independent. Continuous trap distributions other than uniform did not produce satisfactory fits to the data between 2 and 200 v for film XII. For example, if the capture centers were assumed to be a three-dimensional band having spherical energy surfaces, then one expects $j\propto V\exp(V/V_0)^{\frac{1}{2}}$ in the high-voltage region. The resultant parameters from that region then gave a current only $\frac{1}{5}$ of that actually observed in the V^2 region. To insure that the observed currents represented the bulk properties of the films, and that they were not due to surface leakage of the sample or sample holder, currents were also measured with the NESA electrode positive. The currents were representative of the 10^{15} ohm resistance of the sample holder for applied voltages less than 10 v, and increased sharply above that voltage, possibly due to breakdown of the reverse biased NESA contact, but were always more than an order of magnitude less than those shown in Figs. 11–13.

The electrical parameters of the films were obtained from Eqs. (17)–(19) by taking the area of current flow to be 1 cm^2, that being the area of the gold electrode, and the results are given in Table III. At an applied voltage of 200 v, the data indicate that the quasi-Fermi level for holes was still in the uniform distribution of hole capture levels. Using Eq. (11), this requires that the width in energy of the distribution be greater than 0.15 ev. Also, the distribution can at most extend to the valence band edge. Thus, the total density of the hole capture levels observed in the SCLC measurements would be $1.5-9\times10^{14}$ cm^{-3}.

Although the I-V characteristics of SCLC have been interpreted using the model of a uniform distribution in energy of hole capture levels, previous work[9] has used the model of a discrete level, and the exponential rise of current with voltage has been interpreted as the traps-filled limit. The slope of the I-V curve in this high-voltage region, being much less than theory[16] predicts, has been attributed to the presence of more than one level. Although it is very likely that several hole-capture levels exist, the trap-filled limit theory may be readily extended to the case of one filled level separated from nearly empty states by several kT to show that the dependence of current on voltage is unchanged, so long as the Boltzmann approximation is valid for the nearly empty levels. Thus, the rise of current with increasing voltage is very rapid unless the unfilled levels contain nearly as many carriers as the filled level, in which case the current is only an order of magnitude or so less than that which would be obtained by neglecting the filled level altogether. This would predict that a current rising as V^3 to V^5 would approach a V^2 dependence if the applied voltage were doubled. Since no such tendency was observed in this work, the behavior of the current in the high-voltage region requires a continuous distribution in energy of capture levels for successful interpretation, if the traps-filled limit theory is valid.

As a test of this hypothesis, the dependence of current on temperature was measured for film XII at several applied voltages, the results being shown in Fig. 14. At an applied voltage of 13.7 v, the quasi-Fermi level for holes was less than kT above the hole capture levels, and Fermi statistics were used to predict the dependence of current on temperature for the case of a uniform trap distribution. The numerical calculation predicted $I\propto\exp(-0.99\text{ ev}/kT)$ near room temperature, while the measured curve gave an activation energy of 0.95 ev. The agreement is quite satisfactory, since the error could have been caused by an overestimate of the product $N_v\mu_{0p}$ by a factor of 5. The agreement at 120 and 200 v is quite unsatisfactory, however, as the activation energy should have been 0.88 ev at 200 v for the uniform-trap model. In fact, the 0.35 ev dependence strongly suggests a trap-filled limit region in which the Fermi level had passed through a discrete level and was approaching another level which was 0.35 ev above the valence band edge. If the data of film

XII is reevaluated using the model of two discrete levels with a trap-filled-limit voltage of 60 v, then the level dominating the $I \propto V^2$ region would be 0.99 ev above the valence band edge and would have a density of 8.5×10^{13} cm^{-3}. If the level which is filling in the trap-filled limit is placed 0.35 ev above the valence band edge, the theory requires that this level have a density greater than 10^{22} cm^{-3} in order to account for the relatively slow rise of current with voltage at an applied voltage of 200 v. Such a high density of levels is unlikely, even in an amorphous solid.

When the measurements of I vs T were completed, it was noticed that the room temperature currents at 120 and 200 v were about a factor of 2 greater than those shown in Fig. 12. Furthermore, these currents and their temperature dependences were the same regardless of electrode polarities, suggesting that some leakage path might be affecting the measurements. An examination of the sample revealed that three very small areas of the film had crystallized. This was probably caused by localized heating when breakdown occurred at each area, and quite possibly happened when the 200 v were applied to the sample prior to cooling. It is thus felt that the I vs T measurements at 120 and 200 v did not represent the true properties of amorphous selenium, and that the retention of the model of a uniform distribution in energy of the hole-capture centers is permitted.

The low conductivity of 2×10^{-16} ohm^{-1} cm^{-1} observed at room temperature in film XII is much less

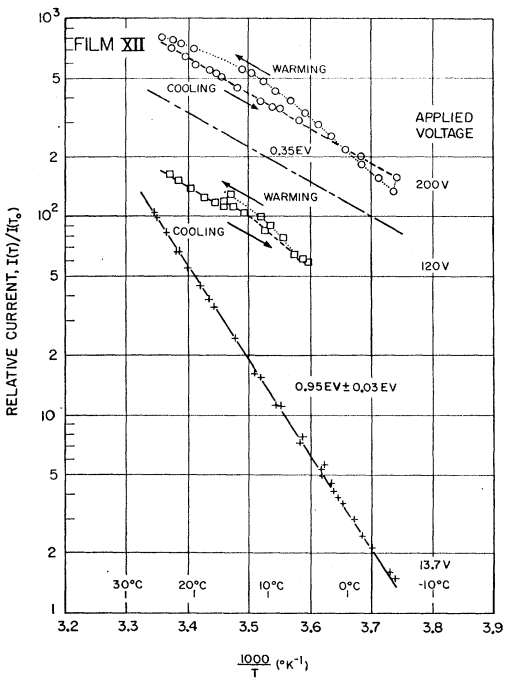

FIG. 14. Dependence of space-charge-limited currents on temperature in an amorphous selenium film having a tellurium hole-injecting contact.

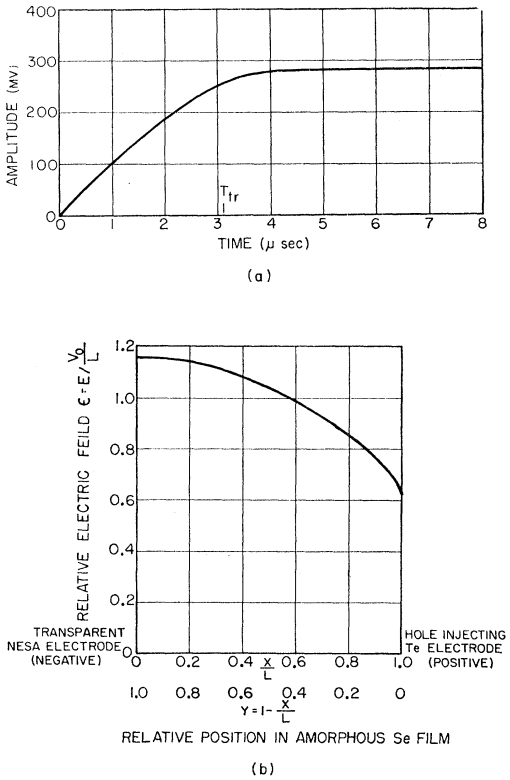

FIG. 15. (a) Pulse shape of drifting electrons and (b) the spatial dependence of the electric field for a space-charge-limited current. Film XII; film thickness, $L=21.3$ μ, applied voltage, $V_0=182$ v.

than previously reported[9] values. It is interesting to note that if the conductivity of liquid selenium[22,23] is extrapolated to 297°K, the result is a conductivity of $1.3-2\times10^{-16}$ ohm^{-1} cm^{-1}. As the band gap and carrier mobilities of semiconducting selenium do depend on temperature, the close agreement between the conductivity of amorphous selenium and that extrapolated from the liquid is surely fortuitous, but it does suggest that the two forms may be electrically similar and that the amorphous films used in this work may have been nearly intrinsic.

Hole drift mobilities and mean-free-drift times in films II and XII agreed with those reported in Sec. IV (A), but the pulses observed for electron drift were distorted and indicated a nonuniform electric field. The pulse shapes could not be attributed to "permanent" capture of the drifting electrons without the use of mean-free times much shorter than those measured in identical films. A typical electron drift pulse, shown in Fig. 15(a), was analyzed using Eqs. (20) and (21) to obtain the spatial dependence of the electric field. As the amplitude of the light pulse had considerable jitter, the total number of injected carriers N_0 was adjusted to give $\int_0^L E(x)dx=V_0$. A mean-free-drift time of $\tau=15$ μsec was assumed for the drifting

[22] H. W. Henkels, J. Appl. Phys. **21**, 725 (1950).
[23] B. Lizell, J. Chem. Phys. **20**, 672 (1952).

electrons. The resulting electric field, shown in Fig. 15(b), has the spatial dependence expected of a SCLC carried by holes which were injected at the anode. However, in view of the uncertainty regarding N_0, the results are only qualitative. The spatial variation of the electric field cannot be explained by any trap-distribution model discussed in this section.

Previous SCLC measurements[8,9] were made on amorphous films which had much higher conductivities than those used in this work; thus the explored regions of the band gap are different and comparison of the results is unjustified.

V. DISCUSSION

Perhaps one of the most interesting results of the work reported here was the excellent agreement of the drift mobilities with those reported by Spear.[6] It is doubtful that the shallow traps which were assumed to limit the drift mobilities are due to impurities, as it is likely that the selenium used in this investigation was purer than that used by Spear and would thus have fewer impurity levels; an indication of the higher purity was given by the conductivities which were orders of magnitude smaller than those reported by Lanyon and Spear.[9] Also, the densities of shallow traps were several orders of magnitude greater than the densities of spectroscopically observable impurities. If these shallow levels are due to imperfections, then their densities would have to be nearly identical in the samples used here and in those used by Spear. As the degree of disorder in evaporated amorphous films should depend on the methods of preparation, that is on evaporation rate, substrate temperature, etc., it is possible that the techniques used were sufficiently alike to produce structurally similar samples. This is quite likely, as the substrate temperatures were uncontrolled in both cases and would thus have been between room temperature and 70°C, above which amorphous Se crystallizes.

A different explanation[3,4] of the low, thermally activated drift mobilities might be that the mean-free path is small compared to an interatomic spacing, and that carriers move by making thermally activated jumps from atom to atom. This model possesses many similarities to the theory of ionic conductivity. Another model[24] might propose that carriers are quite mobile in a chain, but encounter potential barriers, located at chain ends or between adjacent chains, over which the carriers must jump in order to move macroscopically, the jump being assisted by thermal lattice vibrations. Both of the above models might predict a true mobility approximately equal to the drift mobility, but neither can account for the SCLC results without the introduction of deep-hole-capture levels into the model.

Although addition of arsenic to the amorphous films introduced shallow electron traps, in agreement with previous work,[7] the evidence indicates that these levels were not localized at the sites of the As atoms, but were due to a decrease in atomic order caused by the presence of the impurity. As the arsenic did not produce observable hole-capture centers or deep-electron-capture centers, in disagreement with prior results,[7] it is possible that the As atoms were not electrically active. It has been proposed[25] that donor or acceptor impurity levels might not exist in solids in which potential fluctuations, caused by departures from atomic periodicity, were greater than the binding energy of a carrier to the impurity. Thus, some of the group V and VII elements may not be electrically active in amorphous selenium. However, impurities which would produce deep levels could act as donors or acceptors. Imperfections are not barred by the potential fluctuations from electrical activity since they are the actual source of the departures from periodicity.

The low conductivities measured in films of amorphous selenium indicate that the electron- and hole-capture levels observed in drift mobility and SCLC measurements should be neutral in thermal equilibrium, i.e., acceptor-like electron capture levels and donor-like hole-capture levels, for otherwise their high densities would result in high, extrinsic conductivity.

Although SCLC measurements suggest a continuous distribution in energy of deep-hole-capture levels, the measured drift mobilities have not distinguished between discrete and continuous shallow electron and hole traps. However, since these shallow levels have been attributed to imperfections, and since it is doubtful that each imperfection would have an identical environment, a continuous distribution in energy of the shallow traps seems more likely. Their high densities alone suggest that these levels might tend to band and to remove the discrete conduction and valence band edges in a manner similar to impurity banding[26] in Ge and Si, as the densities give mean spacings of 10 to 100 A. At these small distances, wave functions of electrons bound to neighboring imperfections could have appreciable overlap, producing a band. Perturbations due to the random positioning of imperfections in the lattice, coupled with their high densities, would be expected to cause the otherwise sharp conduction or valence band edges to "fuzz out," and possibly to merge with the imperfection levels.

VI. CONCLUSIONS

The band model of a semiconducting solid has been successfully applied to the results of drift mobility and SCLC measurements which were made on a noncrystalline solid. These results have been explained by the introduction of impurity or imperfection levels into the energy gap between a conduction and a valence band

[24] E. Billig, Proc. Phys. Soc. (London) **B65**, 216 (1952).

[25] I. Z. Fisher, J. Solid-State Phys. (USSR) **1**, 192 (1959) [translation: Soviet Phys.—Solid State **1**, 171 (1959)].

[26] F. Blatt, *Solid-State Physics*, edited by F. Seitz and D. Turnbull (Academic Press Inc., New York, 1957), Vol. 4, p. 256.

in the evaporated amorphous selenium films, as shown in Fig. 16. The validity of sharp band edges is somewhat in doubt.

Observed drift mobilities suggested that approximately 10^{19} cm^{-3} electron traps were present in a 0.285-ev region just below the conduction band and that about 10^{21} cm^{-3} hole traps were present in a 0.14-ev portion of the gap immediately above the valence band. The high densities of these levels and the good agreement of the measured drift mobilities with independent results suggest that the shallow traps are due to imperfections produced by the absence of long range order in the amorphous solid. The observed mean-free-drift times of injected carriers indicated the presence of electron- and hole-capture centers which are relatively deep in the energy gap, but did not reveal whether these levels were traps or recombination centers. Since the mean-free-drift times exhibited some variation between samples prepared from selenium of different purities, these capture levels were tentatively assigned to impurities. It has been demonstrated that the addition of arsenic to amorphous selenium produces shallow electron traps by increasing the number of imperfections. No other observable states in the gap were produced by the arsenic and it is possible that the arsenic atoms are electrically inactive due to large, local potential fluctuations in the noncrystalline solid.

Gold and tellurium electrodes have been used to inject holes into amorphous selenium and currents have thus been space charge limited at sufficiently high fields. The observed currents have been explained by assuming that hole-capture centers were distributed uniformly in energy in a region extending downwards from 1 ev above the valence band edge. The densities of these levels were about 10^{15} cm^{-3} ev^{-1} and the width in energy of the distribution was 0.15 to 1 ev. These levels could have been either traps or recombination centers. The drift of photoinjected carriers in the presence of SCLC has been used to probe the electric field in amorphous selenium films. The general spatial dependence of the field agreed with theory, but could not be explained quantitatively. Electrical conductivities of 10^{-14} to 10^{-16} ohm^{-1} cm^{-1} have been measured and were several orders of magnitude smaller than previously measured values. It was suggested that the material was nearly intrinsic. If such was the case, the levels in the gap which affected drift mobilities and SCLC would have to be neutral in order to avoid strongly extrinsic conductivity. The lowest conductivity agreed well with values extrapolated from conductivities of liquid selenium, adding another entry to the growing list of similarities between the amorphous and liquid forms of selenium.

The short-range order in amorphous selenium, brought about by covalent bonding in the chains, has justified the application of band theory which, at present, has been successfully applied to the results of this experimental work as well as previous results. A modification of the usual band theory may be necessary,

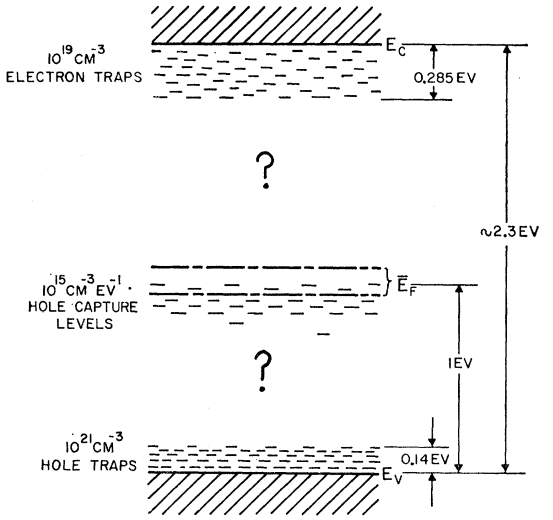

FIG. 16. Population of the band gap in amorphous selenium obtained from drift mobility and space-charge-limited current measurements.

however, if the band edges are not sharp. Indeed, the high densities of shallow traps and the observed drift mobilities have led Bardeen to suggest that a model might apply in which the bands and shallow traps are replaced by continuous distributions in energy, and that electrons or holes could have mobilities which would increase as their energies increased. Thus, both densities of states and mobilities would depend on energy, and both factors would have to be considered when taking statistical averages over energy. It appears that the current major problem is that of establishing a satisfactory charge transport mechanism. As the proposed true mobilities seem to indicate a mean-free path less than an interatomic distance, a straightforward extension of existing theory is unjustified. The existence of thermally-activated true mobilities has not been ruled out. Indeed, if the true mobilities possess a temperature dependence of $\exp(-E/kT)$, the quantitative conclusions of this work regarding trap densities and positions in the energy gap are in error, since any temperature variation of true mobility was neglected. Thus, in order to establish a model for the electrical properties of amorphous selenium, measurement of the magnitude and temperature dependence of true mobilities is clearly required. The photoconductive Hall effect[27] technique could well produce such information.

The similarities between amorphous and liquid selenium encourage extension of the measurements reported here to the liquid. In particular, drift-mobility measurements on the liquid might be fruitful, as the viscosities[28] of liquid selenium suggest that the atomic order is strongly temperature dependent. Thus, if the low, thermally-activated drift mobilities are associated

[27] A. G. Redfield, Phys. Rev. **94**, 526 (1954).
[28] S. Dobinski and J. Wesolowski, Bull. acad. polon. **49A**, 7 (1937).

with the absence of long-range order, the temperature dependences of these mobilities in the liquid should differ from those reported for amorphous selenium.

The examinations of electrical and optical properties of noncrystalline and low mobility semiconductors are currently in an interesting phase, and future work should contribute significantly toward a more complete understanding of the physics of solids.

ACKNOWLEDGMENTS

It is indeed a pleasure for the author to acknowledge the guidance and support given by J. Bardeen during the course of this work. The supply of samples, advice, and cooperation, which have been generously furnished by F. A. Schwertz and his associates of the Xerox Corporation, is sincerely appreciated. The writer wishes to thank both F. C. Brown for the many instructive discussions concerning drift-mobility measurement and R. K. Swank for the discussions which contributed significantly to the development of the pulsed light source. The fellowships which were granted the author during a portion of this work by Texas Instruments, Inc. and the National Science Foundation are gratefully acknowledged.

PHYSICAL REVIEW VOLUME 125, NUMBER 4 FEBRUARY 15, 1962

Magnetoacoustic Effects in Tilted Magnetic Fields*†

HAROLD N. SPECTOR‡
Institute for the Study of Metals and Department of Physics, University of Chicago, Chicago, Illinois
(Received July 3, 1961; revised manuscript received October 11, 1961)

We have shown for the cases of a free-electron gas, the two-spherical-band model, and the model of majority and minority carriers that certain portions of the Fermi surface can be mapped in detail. This can be done by using geometric resonances in the sound attenuation in tilted magnetic fields, and the drift velocity of the carriers along the magnetic field can simultaneously be determined. For this to be possible, $\omega\tau$ must exceed unity and the Fermi velocity must not exceed the sound velocity by more than a factor of 100. Then the diameters of all the orbits, not merely the extremal orbits, can be measured and the drift velocity along the magnetic field determined as well. The general features of the phenomena considered do not prove dependent on the particular models used in our calculations. In addition to the results specifically pertaining to tilted fields, we have found that when the assumptions of equal effective masses and relaxation times are dropped for a two-band model of a semimetal, the contribution of the two types of carriers to the ultrasonic absorption is additive. On examining the contribution to the absorption for a model of majority and minority carriers, we have found, also, that the minority carriers dominate the attenuation when they are in the region of geometric resonances.

I. INTRODUCTION

IN the past few years, experiments have been performed on magnetoacoustic absorption in metals and semimetals at low temperatures.[1–7] Several interesting phenomena have been observed which prove useful in determining the electronic structure of metals. In a transverse magnetic field, there are oscillations in the ultrasonic attenuation with magnetic field.[8–11] These oscillations occur when the cyclotron diameter of an extremal orbit is equal to an integral number of wavelengths. Also, in the high field limit, when the magnetic field is tilted from a direction perpendicular to the direction of propagation of the sound wave, there is an increase in the attenuation.[12] This increase occurs when the carriers drifting along the field with the maximum velocity remain in exact phase with the sound wave. The extremal dimensions of the Fermi surface can be obtained from the periods of the magnetoacoustic oscillations while the Fermi velocity can be determined from the critical angle of tilt at which the increase in attenuation begins.

The possibility of combining the tilt effect and the

* Submitted in partial satisfaction of the requirements for the degree of Ph.D. in Physics, University of Chicago.

† Supported in part by the National Science Foundation, and the Office of Naval Research.

‡ Shell Oil Predoctoral Fellow, 1960–61.

[1] R. W. Morse and J. D. Gavenda, Phys. Rev. Letters **2**, 250 (1959).

[2] R. W. Morse, A. Myers, and C. T. Walker, Phys. Rev. Letters **4**, 605 (1960).

[3] H. E. Bommel, Phys. Rev. **100**, 758 (1955); W. P. Mason and H. E. Bommel, J. Acoust. Soc. Am. **28**, 930 (1956).

[4] T. Olsen, Phys. Rev. **118**, 1007 (1960).

[5] B. W. Roberts, Phys. Rev. **119**, 1889 (1960).

[6] A. A. Galkin and A. P. Korolyuj, J. Exptl. Theoret. Phys. (USSR) **38**, 1688 (1960) [translation: Soviet Phys.—JETP **11**, 1218 (1960)].

[7] D. H. Reneker, Phys. Rev. **115**, 303 (1959).

[8] M. H. Cohen, M. J. Harrison, and W. A. Harrison, Phys. Rev. **117**, 937 (1960).

[9] T. Kjeldaas and T. Holstein, Phys. Rev. Letters **2**, 340 (1959).

[10] A. B. Pippard, Proc. Roy. Soc. (London) **A257**, 165 (1960).

[11] V. L. Gurevich, J. Exptl. Theoret. Phys. (USSR) **37**, 71 (1959) [translation: Soviet Phys.—JETP **10**, 51 (1960)].

[12] H. N. Spector, Phys. Rev. **120**, 1261 (1960).